IEEE Access
Multidisciplinary ⋮ Rapid Review ⋮ Open Access Journal

Received 3 October 2023, accepted 9 October 2023, date of publication 16 October 2023, date of current version 24 October 2023.

Digital Object Identifier 10.1109/ACCESS.2023.3324891

RESEARCH ARTICLE

MIMO-Based Physical Layer Evaluation on IEEE 802.11bd

SHUTING GUO[1,2], DANIEL N. ALOI[1], (Senior Member, IEEE), JIA LI[1], (Senior Member, IEEE), AND HONGMEI ZHAO[2]

[1]Department of Electrical and Computer Engineering, Oakland University, Rochester, MI 48309, USA
[2]College of Electrical and Information Engineering, Zhengzhou University of Light Industry, Zhengzhou, Henan 450002, China

Corresponding author: Daniel N. Aloi (aloi@oakland.edu)

ABSTRACT To enable vehicle-to-everything (V2X) communications, both the dedicated short-range communications (DSRC) and the cellular V2X (C-V2X) involved in the radio access technologies (RATs) are experiencing extensive development to support advanced vehicular applications and scenarios. Compared with the C-V2X whose effective reliability and scalability are still to be completely verified, the DSRC maintains its superiority due to the extensive safety-related field trials performed worldwide. Furthermore, IEEE 802.11bd, the next-generation V2X (NGV) standard for the vehicular ad hoc networks (VANETs) in the DSRC, is expected to greatly improve the performance compared to IEEE 802.11p with new physical layer (PHY) and medium access control (MAC) technologies. Hence, aimed to obtain the complete PHY evaluation on IEEE 802.11bd in terms of the packet error rate (PER), the packet reception ratio (PRR), the effective data rate, and the packet inter-arrival time (IAT), the various antenna configurations, vehicle-to-vehicle (V2V) scenarios, packet sizes, and modulation and coding schemes (MCSs) are investigated and compared in a full PHY simulation. The results indicate that the multiple-input multiple-output (MIMO) configuration is the most advantageous technique in decreasing the PER, increasing the PRR and the transmission coverage, elevating the output effective data rate, and reducing the output packet IAT in contrast with the single-input multiple-output (SIMO), multiple-input single-output (MISO), and single-input single-output (SISO) configurations at the farther distance. The urban non-line-of-sight (NLOS) scenario experiences the slightly better quality of communication and is more robust than the highway NLOS scenario. Both the packet size and the MCS need to be selected properly to satisfy the high-reliability, high-throughput, or low-latency requirements.

INDEX TERMS IEEE 802.11bd, V2X, MIMO, physical layer evaluation.

I. INTRODUCTION

Vehicle-to-everything (V2X) communications involved in the intelligent transportation system (ITS) have the potential and ability to not only improve the road safety, but also enhance the traffic management, energy savings, and air protection [1], [2]. In 1999, the 75 MHz licensed spectrum in the 5.9 GHz frequency band, 5.850 − 5.925 GHz, is designated by the U.S. Federal Communications Commission (FCC) for the ITS to support the V2X communications including both the vehicle-to-vehicle (V2V) and the vehicle-to-infrastructure (V2I) communications [3], [4]. Since then, the research effort worldwide has been focused on the vehicular communications to address multiple challenges in the ITS, such as connected autonomous driving, cooperative maneuvering, smart navigation, and safety to vulnerable road users [5].

To enable the V2X communications, both the dedicated short-range communications (DSRC) and the cellular V2X (C-V2X) included in the radio access technologies (RATs) are experiencing extensive development to support advanced vehicular applications and scenarios with the high-reliability, high-throughput, and low-latency requirements [1]. The DSRC operates primarily in the 5.9 GHz frequency band, which has been allocated for the ITS applications in the U.S., Europe, and many other countries [6]. The C-V2X can

The associate editor coordinating the review of this manuscript and approving it for publication was Barbara Masini.

operate in the 5.9 GHz frequency band as well as in the licensed bands of the cellular operators [1], [7].

As the basic standard for the vehicular ad hoc networks (VANETs) in the DSRC, IEEE 802.11p allows direct communication between two user devices without the use of a base station [8]. Moreover, IEEE 802.11bd, the next-generation V2X (NGV) standard, is expected to greatly improve the performance compared to IEEE 802.11p with new physical layer (PHY) and medium access control (MAC) technologies [9], [10]. On the other hand, the 3rd Generation Partnership Project (3GPP) introduces advanced features of V2X communication in the long-term evolution (LTE) in Release 14 as an alternative to 802.11p based on the cellular technologies [11], [12]. Furthermore, the new radio V2X (NR-V2X), the next-generation C-V2X which was released in Release 16 including the first V2X standard based on the 5th generation (5G) NR air interface, enables advanced features on the 5G NR air interface to support connectivity and autonomous driving use cases with strict requirements [12], [13].

As a main competitor to the DSRC, the C-V2X has the potential to interact with the 5G-and-beyond cellular technologies so that the vehicular communication is not limited to the V2V and V2I communications [14], [15], [16]. However, the DSRC remains its superiority due to the extensive safety-related field trials performed worldwide compared with the C-V2X whose effective reliability and scalability are still to be completely verified [17]. Although IEEE 802.11p is designed as the key standard of wireless access in vehicular environments (WAVE) architecture [18] for the DSRC and can provide safety and service applications for the ITS in the vehicular communications [19], it fails to fulfill requirements on very low frame transmission delay and packet loss ratio imposed by modern V2X applications [9]. Hence, IEEE 802.11bd was proposed as the amendment of IEEE 802.11p with the evolution for IEEE-based V2X communications by enhancing the reliability, throughput, and transmission range [20], [21], [22].

II. RELATED WORKS

The following several works are devoted to the performance assessment on the DSRC and the C-V2X standards.

It is pointed out in [23] that both C-V2X technologies can support all the considered V2I services without any limitations based on the simulation which benchmarks their performance deployed for V2I communications in an urban scenario. However, it is also mentioned in [24] that, compared to the DSRC technology which can achieve a less end-to-end delay and a higher packet delivery ratio (PDR) in the investigated V2I communication scenarios, the LTE technology manifests the worse performance which imposes the limitation on its suitable applications. Moreover, according to the system-level simulation implemented under the highway scenario in [25], the DSRC performs better than the LTE with the less and stable data packet delay with the higher vehicle density. Meanwhile, as the variant standard of DSRC in Europe, ITS-G5 is compared with the LTE-V2X under the real-life highway environment in [26] and provides the lower latency for both V2I and V2V scenarios. In addition, based on the simulation fulfilled under the realistic urban scenarios in [27], the ITS-G5 outperforms the LTE-V2X on which the concurrent applications are scheduled. Furthermore, depending on the simulation realized under the urban scenario in [28], IEEE 802.11bd presents the better performance in terms of the packet error rate (PER), packet reception ratio (PRR), data rate, and packet inter-arrival time (IAT) in contrast with IEEE 802.11p.

However, certain gaps in the existing works on IEEE 802.11bd need to be compensated to achieve its better performance evaluation. The parameters, performance, and mechanism of IEEE 802.11bd are introduced conceptually in [1] without the support of any simulation results. Aimed at the estimation on the reliability requirement, the PER is the unique metric in [29] for the PHY simulation. Focused on the highway line-of-sight (LOS) and non-line-of-sight (NLOS) scenarios, the PER and PRR used in [30] cannot realize the investigation on PHY performance related to the throughput and latency. Even if the complete PHY metrics, PER, PRR, data rate, and packet IAT, are utilized in [28] for the PHY evaluation, the simulation is only implemented on a single-input single-output (SISO) channel for the urban NLOS scenario, without the consideration of a multiple-input multiple-output (MIMO) channel and any other V2V scenarios. When the PER and throughput are adopted in [21] for the simulation on the 1×1, 2×1, and 2×2 configurations in all V2V scenarios, the investigation on the 1×2 system is still absent.

The contributions of the proposed work lie in the following aspects. Firstly, the complete PHY metrics, including the PER, PRR, effective data rate, and packet IAT, are employed to accomplish the full evaluation on the PHY performance of IEEE 802.11bd. Secondly, all the antenna configurations, including the SISO, single-input multiple-output (SIMO), multiple-input single-output (MISO), and MIMO systems, are studied to explore their features and merits. Finally, both V2V channel models for the NLOS scenarios, both the ultra-reliable low-latency communications (URLLC) and enhanced mobile broadband (eMBB) applications, and different modulation and coding schemes (MCSs) are covered to respectively analyze the impact of Doppler effect, packet size, and MCS on the PHY performance.

The detailed comparisons between the existing literature and this work are listed in Table 1.

The remainder of the paper is organized as follows. The overview of IEEE 802.11bd, antenna configuration, V2V channel model, and the related PHY metrics are provided in Section III. The simulation on IEEE 802.11bd, which is fulfilled according to the PHY metrics including the PER, PRR, effective data rate, and packet IAT with the various antenna configurations, packet sizes, and MCSs in both the urban NLOS and the highway NLOS scenarios, is presented and analyzed in Section IV. Finally, the paper is summarized in Section V.

TABLE 1. Comparison between existing literature and this work.

Source	PHY Metric				Parameter			
	PER	PRR	Effective Data Rate	Packet IAT	Antenna Configuration	V2V Scenario	Packet Size	MCS
[1]	No	No	No	No	N/A	N/A	N/A	N/A
[29]	Yes	No	No	No	SISO	Rural LOS Urban LOS Urban NLOS Highway LOS Highway NLOS	300 bytes	MCS 0 MCS 3
[30]	Yes	Yes	No	No	SISO	Highway LOS Highway NLOS	300 bytes	MCS 1
[28]	Yes	Yes	Yes	Yes	SISO	Urban NLOS	100 bytes 1500 bytes	MCS 1/MCS 0 MCS 5
[21]	Yes	No	Yes	No	SISO MISO MIMO	Rural LOS Urban LOS Highway LOS Urban NLOS Highway NLOS	100 bytes 300 bytes	MCS 1 MCS 4
This Work	**Yes**	**Yes**	**Yes**	**Yes**	**SISO MISO SIMO MIMO**	**Urban NLOS Highway NLOS**	**100 bytes 1500 bytes**	**MCS 1 MCS 5**

III. THEORIES AND TECHNOLOGIES

A. IEEE 802.11BD

Aimed at improving the communication reliability, the transmission range, and the throughput compared to the legacy IEEE 802.11p standard, IEEE 802.11bd is proposed as the NGV standard which defines modifications to both the IEEE 802.11 MAC and PHY for V2X communications for 5.9 GHz frequency band and optionally in the 60 GHz band [31]. The advancements are expected to achieve at least twice the MAC throughput of 802.11p with relative speeds up to 500 km/h, at least 3 dB lower sensitivity level and thus twice the communication range of 802.11p, and interoperability, coexistence, backward compatibility, and fairness with 802.11p devices [1], [31], [32].

In comparison with the Wi-Fi standards which have been developed for the low-mobility applications, the DSRC was designed for the high-mobility vehicular networks and the corresponding enhancements were introduced to make the DSRC suitable for such environments [1]. Since 20 MHz IEEE 802.11ac orthogonal frequency-division multiplexing (OFDM) numerology is shown as a good choice for 10 MHz DSRC channel for its efficiency and Doppler resilience [33], the bandwidth of 802.11bd is reduced to 10 MHz by halving the 20 MHz bandwidth of 802.11ac and thus all the OFDM timing parameters are doubled in order to make the signal more robust against fading and more tolerant to multipath effects of signals in a vehicular environment. The comparison of the PHY parameters on 802.11p, 802.11ac, and 802.11bd are shown in Table 2 [5], [8], [28] where OFDM symbol duration is provided with guard interval (GI) included.

To improve the spectral efficiency and reduce the inter-symbol interference (ISI) caused by the multipath fading, the OFDM modulation scheme is adopted in the PHY of IEEE 802.11bd. In the multicarrier scheme, a high-data-rate information stream is split into several parallel low-data-rate sub-streams which are then transmitted by modulating onto a set of orthogonal subcarriers in the OFDM transmitter for efficient data transmission [34], [35]. Since the channel delay spread becomes significantly shorter than the OFDM symbol period which has been increased in the parallel transmission, the communication becomes less sensitive to the ISI and the channel equalization in the receiver for the frequency-flat fading becomes easier than that in the frequency-selective fading [36]. Accordingly, channel fading can be mitigated significantly by converting a wideband frequency-selective fading channel into numerous narrowband flat-fading subchannels [37], [38]. A single OFDM symbol is composed of a total of 64 subcarriers, including 52 data subcarriers, 4 pilot subcarriers, and 8 null subcarriers [8]. Hence, a 64-point inverse fast Fourier transform (IFFT) and a 64-point fast Fourier transform (FFT) are utilized in the transmitter and receiver respectively so that the OFDM can be well integrated into current chip sets [39].

In addition to a preamble located at the beginning of a frame which is used for the initial channel estimation, midambles, which are introduced in between the OFDM data symbols periodically, will help in channel tracking so that accurate channel estimates are obtained for all data symbols [1]. With the channel update based on an appropriate periodicity of midambles, the fast variation of the channel can be limited within each midamble periodicity and the PER at the receiver can be effectively decreased [33]. Although the denser midambles can lead to better channel estimation and lower PER, the throughput will also be reduced since the packet duration is increased with the more frequent insertion of midambles [21]. Hence, midamble periodicity should be properly determined from three candidates, 4,

TABLE 2. PHY comparison on IEEE 802.11p, IEEE 802.11ac, and IEEE 802.11bd.

PHY Parameter	IEEE 802.11p	IEEE 802.11ac	IEEE 802.11bd
Data Subcarriers	48	52	52
Pilot Subcarriers	4	4	4
Null Subcarriers	12	8	8
Total Subcarriers	64	64	64
Channel Bandwidth	10 MHz	20 MHz	10 MHz
Subcarrier Spacing	10 MHz/64=156.25 KHz	20 MHz/64=312.5 KHz	10 MHz/64=156.25 KHz
OFDM Symbol Duration	8 µs (1.6 µs GI)	4 µs (800 ns GI), 3.6 µs (400 ns GI)	8 µs (1.6 µs GI)

8, and 16 OFDM symbols [40], in terms of modulation, error control, Doppler spread, and so on [1]. Moreover, the low-density parity-check (LDPC) coding is exploited as the forward error correction (FEC) coding technique to replace the binary convolutional coding (BCC) in IEEE 802.11p [32]. With the combination of midamble and LDPC, the prominent signal-to-noise ratio (SNR) gain and Doppler mitigation can be achieved [33].

The MCS 0-9 of 10 MHz IEEE 802.11bd are derived from 20 MHz IEEE 802.11ac, whereas MCS 10 is the same as MCS 0 except that the dual carrier modulation (DCM) mode is adopted [5]. Depending on the receiver distance, channel conditions, and quality of service (QoS) requirement, an appropriate MCS is selected for transmission from all the possible MCSs summarized in Table 3 [40] where the midamble periodicity is 4 OFDM symbols for all MCSs. Accordingly, the theoretical data rate from 3.25 Mbps to 39 Mbps can be achieved as shown in Table 3. As the half of data rate in 20 MHz IEEE 802.11ac, the theoretical data rate of 10 MHz IEEE 802.11bd is only available for MCS 0-8. Moreover, MCS 9 of 10 MHz IEEE 802.11bd is not valid since the number of data bits per OFDM symbol is not an integer.

B. ANTENNA CONFIGURATION

According to the number of transmit antennas and receive antennas, wireless communication can be classified into SISO, MISO, SIMO, and MIMO systems, where the input and output are with respect to the channel between the transmitter and the receiver [37]. In addition to the time and frequency dimensions which are exploited in the conventional single-antenna configuration, i.e., SISO system, the spatial dimension is also developed in the multi-antenna configurations, i.e., MISO, SIMO, and MIMO systems. A linear time-invariant channel model is assumed to simulate the combined effects of multipath propagation and frequency selectivity.

In a SISO system without signal redundancy, deep-fading signals are beyond detection. However, with multiple transmit antennas and/or multiple receive antennas, signals can be transmitted and/or received with diversity to combat channel fading. Hence, the multi-antenna technology can greatly enhance the performance of wireless communication systems without the penalty in bandwidth and power [37], [41].

The system model of a MIMO system with N_{T} transmit antennas and N_{R} receive antennas is illustrated in Fig.1 [42], [43].

The jth receive antenna observes the superposition [44]

$$y^{(j)}(t) = \sum_{i=1}^{N_{\mathrm{T}}} \int_{-\infty}^{\infty} h^{(j,i)}(\tau) x^{(i)}(t-\tau) d\tau + v^{(j)}(t) \quad j = 1, \cdots, N_{\mathrm{R}} \tag{1}$$

where $x^{(i)}(t)$ is the signal transmitted by the ith transmit antenna, $h^{(j,i)}(t)$ is the impulse response from the ith transmit antenna to the jth receive antenna, and $v^{(j)}(t)$ is the assumed additive white Gaussian noise (AWGN) at the jth receiver which is independent of the noise at the other receivers.

For the notational and analytical reasons, the $N_{\mathrm{R}} \times 1$ receive signal vector and noise vector are defined respectively as

$$\mathbf{y}(t) = \begin{bmatrix} y^{(1)}(t) \\ \vdots \\ y^{(N_{\mathrm{R}})}(t) \end{bmatrix} \tag{2}$$

$$\mathbf{v}(t) = \begin{bmatrix} v^{(1)}(t) \\ \vdots \\ v^{(N_{\mathrm{R}})}(t) \end{bmatrix} \tag{3}$$

the $N_{\mathrm{T}} \times 1$ transmit signal vector as

$$\mathbf{x}(t) = \begin{bmatrix} x^{(1)}(t) \\ \vdots \\ x^{(N_{\mathrm{T}})}(t) \end{bmatrix} \tag{4}$$

and the $N_{\mathrm{R}} \times N_{\mathrm{T}}$ normalized channel matrix as

$$\mathbf{H}(t) = \begin{bmatrix} h^{(1,1)}(t) & h^{(1,2)}(t) & \cdots & h^{(1,N_{\mathrm{T}})}(t) \\ h^{(2,1)}(t) & h^{(2,2)}(t) & \cdots & h^{(2,N_{\mathrm{T}})}(t) \\ \vdots & \vdots & \ddots & \vdots \\ h^{(N_{\mathrm{R}},1)}(t) & h^{(N_{\mathrm{R}},2)}(t) & \cdots & h^{(N_{\mathrm{R}},N_{\mathrm{T}})}(t) \end{bmatrix} \tag{5}$$

Hence, the MIMO transmit-receive relationship can be written compactly as [44], [45]

$$\mathbf{y}(t) = \int_{-\infty}^{\infty} \mathbf{H}(\tau) \mathbf{x}(t-\tau) d\tau + \mathbf{v}(t) \tag{6}$$

Let $\mathbf{y}[n] = \mathbf{y}(nT)$, $\mathbf{x}[n] = \mathbf{x}(nT)$, and $\mathbf{v}[n] = \mathbf{v}(nT)$, where T is the sampling period, then the discrete-time

TABLE 3. MCS options, data rate, and transmission latency of 10MHz IEEE 802.11bd.

MCS	Modulation	Coding Rate	Theoretical Data Rate (Mbps)	Actual Data Rate (Mbps)		Transmission Latency (ms)	
				100 bytes	1500 bytes	100 bytes	1500 bytes
0	BPSK	1/2	3.250	1.923	2.538	0.416	4.728
1	QPSK	1/2	6.500	3.030	4.967	0.264	2.416
2	QPSK	3/4	9.750	3.704	7.282	0.216	1.648
3	16-QAM	1/2	13.00	4.348	9.494	0.184	1.264
4	16-QAM	3/4	19.50	4.762	13.64	0.168	0.880
5	64-QAM	2/3	26.00	5.556	17.44	0.144	0.688
6	64-QAM	3/4	29.25	5.556	19.23	0.144	0.624
7	64-QAM	5/6	32.50	5.556	20.83	0.144	0.576
8	256-QAM	3/4	39.00	5.882	24.19	0.136	0.496
9	256-QAM	5/6	N/A	N/A	N/A	N/A	N/A
10	BPSK with DCM	1/2	N/A	1.099	1.284	0.728	9.344

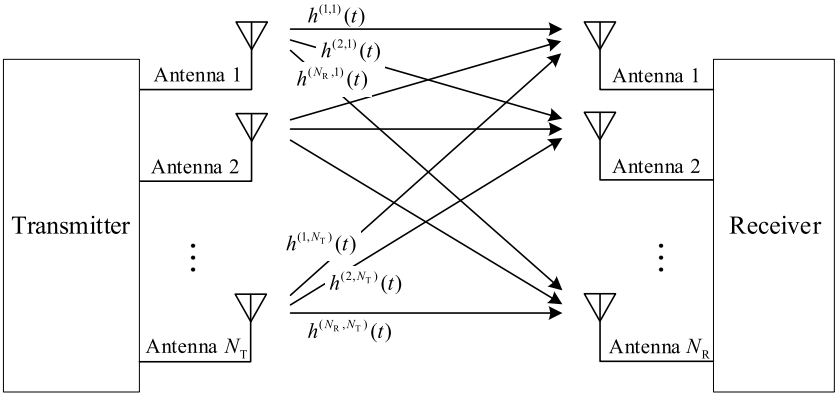

FIGURE 1. MIMO system model.

multivariate impulse response at tap l is denoted as $\mathbf{H}[l]$ where $[\mathbf{H}[l]]_{j,i}$ is obtained by filtering and sampling $h^{(j,i)}(t)$. Hence, the discrete-time transmit-receive MIMO relationship becomes [44], [46]

$$\mathbf{y}[n] = \sum_{l=0}^{L} \mathbf{H}[l]\mathbf{x}[n-l] + \mathbf{v}[n] \tag{7}$$

where L is the number of channel taps. If $L = 0$, the frequency-selective MIMO relationship in (7) reduces to the frequency-flat MIMO relationship [47], [48], [49]

$$\mathbf{y}[n] = \mathbf{H}\mathbf{x}[n] + \mathbf{v}[n] \tag{8}$$

MIMO systems can be used either to increase the data transmission rate by sending different bit streams independently in the spatial multiplexing or to obtain the reliable communication by sending the same bit stream over independent paths in the spatial diversity [50]. To compromise between maximizing the multiplexing gain in order to achieve the best spectral efficiency and maximizing the diversity gain so as to increase the link reliability against fading, the trade-off between the multiplexing gain and the diversity gain needs to be leveraged [42].

The multiplexing gain r satisfies the relationship with

$$0 \le r \le \min(N_T, N_R) \tag{9}$$

then the optimal diversity gain can be calculated as [35], [42], [43]

$$d_{opt}(r) = (N_T - r)(N_R - r) \tag{10}$$

C. V2V CHANNEL MODEL

Based on different measurement campaigns implemented in five common V2V scenarios, the V2V channel models are derived in [51] for the performance evaluation and the corresponding parameters are shown in Table 4 where the power, delay, and Doppler frequency of the LOS path and the first several NLOS paths for each scenario are listed.

1) RURAL LOS SCENARIO

In an open environment without other vehicles, buildings, and large fences, the LOS communication is dominant between two vehicles with a strong LOS component and several weak multipath components.

2) URBAN APPROACHING LOS SCENARIO

During the communication between two approaching vehicles in an urban street with buildings nearby, the stronger multipath components, which are still much weaker than the LOS component, can be observed compared to the rural LOS scenario.

3) URBAN CROSSING NLOS SCENARIO

When the communication takes place between two vehicles approaching an urban blind intersection with other traffic, buildings, and fences present, the NLOS communication becomes predominant with the much stronger multipath components and the strong fading occurs due to the absence of dominant LOS component as well as the small difference in power among multipath components [29].

4) HIGHWAY LOS SCENARIO

Confronted with the communication between two vehicles following each other on multilane inter-region roadways, the LOS communication is still significant even if the signs, overpasses, hillsides, and other traffic are present. However, a higher Doppler shift can be observed due to the higher differential speed between vehicles.

5) HIGHWAY NLOS SCENARIO

Similar to the highway LOS scenario except that a truck is in between communicating vehicles and blocking the LOS path, the NLOS communication is prominent with the much stronger multipath components and the fast fading exists because of the high Doppler spread [29].

With the introduction of scenarios containing buildings, fences, and other vehicles, the NLOS communication becomes indispensable in addition to the LOS communication. Because of these obstacles, the signal propagates through multiple paths by means of reflection, diffraction, refraction, and scattering mechanisms. Consequently, the power of the received signal fluctuates in space (due to angle spread) and/or frequency (due to delay spread) and/or time (due to Doppler spread) through the random superposition of the impinging multipath components [52]. Hence, in addition to the typical impairments of the wireless channel in the LOS propagation conditions including noise, co-channel interference, path loss, and scarce available bandwidth, there exist other detrimental impairments in the NLOS propagation environments such as multipath fading, which consists of the severe fluctuations in the received signal [53]. Since the LOS environment has less multipath components than the NLOS environment, it is expected that MIMO can bring a larger gain in the data rate for the NLOS environment compared to the LOS environment [54].

D. PHY METRIC

1) TRANSMISSION LATENCY

The transmission latency, i.e., packet duration, is the time required to transmit an IEEE 802.11bd packet to the air interface [10], [28]. It can be obtained as [5], [10]

$$T_{\text{tx}}^{\text{11bd}} = T_{\text{pre}}^{\text{11bd}} + T_{\text{AIFS}}^{\text{11bd}} + T_{\text{sym}}^{\text{11bd}} \cdot N_{\text{sym}}^{\text{11bd}} + T_{\text{sym}}^{\text{11bd}} \cdot N_{\text{ma}} \tag{11}$$

where $T_{\text{pre}}^{\text{11bd}} = 80$ µs is the preamble duration, $T_{\text{AIFS}}^{\text{11bd}} = 32$ µs is the arbitrary inter-frame space (AIFS) for priority data which is set as the short inter-frame space (SIFS) for simplicity, $T_{\text{sym}}^{\text{11bd}} = 8$ µs is the OFDM symbol duration, and $N_{\text{sym}}^{\text{11bd}}$ is the number of OFDM symbols defined as

$$N_{\text{sym}}^{\text{11bd}} = \left\lceil \frac{P_{\text{b}} \cdot 8}{N_{\text{sd}}^{\text{11bd}} \cdot R^{\text{11bd}} \cdot N_{\text{bpscs}}^{\text{11bd}}} \right\rceil \tag{12}$$

where P_{b} is the packet size in bytes, $N_{\text{sd}}^{\text{11bd}} = 52$ is the number of data subcarriers in an OFDM symbol, R^{11bd} is the coding rate, $N_{\text{bpscs}}^{\text{11bd}}$ is the coded bits per subcarrier which equals 0.5 for MCS 10, and $\lceil \cdot \rceil$ is a ceiling function used to round up values to the nearest integer. Moreover, N_{ma} is the number of OFDM symbols used for midamble which is obtained as [5], [40]

$$N_{\text{ma}} = \left\lfloor \frac{N_{\text{sym}}^{\text{11bd}} - 1}{T_{\text{ma}}} \right\rfloor \tag{13}$$

where T_{ma} is the midamble periodicity which is specified as 4 OFDM symbols for all MCSs to obtain the lowest PER by means of the densest midamble insertion, and $\lfloor \cdot \rfloor$ is a floor function used to round down values to the nearest integer.

The transmission latencies described in IEEE 802.11bd are calculated with the 100-byte and 1500-byte packets respectively which are listed in Table 3.

2) THEORETICAL DATA RATE AND ACTUAL DATA RATE

The theoretical data rates for IEEE 802.11bd are obtained by dividing the data bits carried by an OFDM symbol with the duration of the OFDM symbol, as illustrated in Table 3. However, in addition to the data transmission, the transmitted PHY frame also contains a preamble and one or more midambles in each packet, and at least one inter-frame space (IFS) between two consecutive packet transmissions [5]. Hence, the actual data rate is calculated in terms of payload P_{b} and transmission latency $T_{\text{tx}}^{\text{11bd}}$ as [5], [10].

$$\Gamma^{\text{11bd}} = \frac{P_{\text{b}} \cdot 8}{T_{\text{tx}}^{\text{11bd}}} \tag{14}$$

With a very large packet size, the packet duration is much larger than the overhead and thus generates an actual data rate which is closer to the theoretical data rate. Nevertheless, the overhead can have an incredible impact on the applications with very small packet size and thus results in a significant decrease of the actual data rate from the theoretical data rate [5], [28]. The actual data rates provided in IEEE 802.11bd are computed with the 100-byte and 1500-byte packets respectively and presented in Table 3.

IV. SIMULATION AND RESULTS

Based on the simulation of full PHY modeling in a MATLAB-based framework, the PHY performance of IEEE 802.11bd is evaluated in various V2V channel models [51] which emulate the real-world scenarios.

Since the NLOS scenario which is very challenging for the DSRC standards leads to the significant degradation on the communication performance [55], and the MIMO technique is more favorable for the NLOS scenario, whose multipath

TABLE 4. V2V channel model parameters.

V2V Scenario	Power (dB)	Delay (ns)	Doppler (Hz)
Rural LOS	[0 -14 -17]	[0 83 183]	[0 492 -295]
Urban Approaching LOS	[0 -8 -10 -15]	[0 117 183 333]	[0 236 -157 492]
Urban Crossing NLOS	[0 -3 -5 -10]	[0 267 400 533]	[0 295 -98 591]
Highway LOS	[0 -10 -15 -20]	[0 100 167 500]	[0 689 -492 886]
Highway NLOS	[0 -2 -5 -7]	[0 200 433 700]	[0 689 -492 886]

TABLE 5. Simulation parameters.

Parameter	IEEE 802.11bd
Transmit Power	23 dBm
Tx Antenna Gain	3 dB
Rx Antenna Gain	3 dB
Reference Path Loss	47.86 dB (at 1 m)
Path-loss Exponent	2.75
Noise Power	-104 dBm
Noise Figure	9 dB
Packet Size	100 bytes (URLLC), 1500 bytes (eMBB)
V2V Channel Model	Urban NLOS, Highway NLOS
Channel Bandwidth	10 MHz
Carrier Frequency	5.9 GHz

components are more rich compared to the LOS scenario, to combat the multipath fading [54], both the modeled NLOS scenarios, the urban NLOS and the highway NLOS scenarios, are studied to explore the availability and effectiveness of various IEEE 802.11bd applications. The simulation parameters are summarized in Table 5.

The path loss is defined in the log-distance path-loss model as [28], [56]

$$\mathrm{PL}(d) = \mathrm{PL}(d_0) + 10\alpha \log_{10}(d) \tag{15}$$

where d is the distance in meters between the transmitter and the receiver, α is the path-loss exponent, and $\mathrm{PL}(d_0)$ is the reference path loss at $d_0 = 1$ m obtained as [57]

$$\begin{aligned}\mathrm{PL}(d_0) &= 10\log_{10}(\frac{4\pi}{\lambda})^2 d_0^{\alpha} = 10\log_{10}(\frac{4\pi}{\lambda})^2 \\ &= 10\log_{10}(\frac{4\pi}{c/f_c})^2 = 47.86 \text{ dB}\end{aligned} \tag{16}$$

where λ is the wavelength, $c = 3 \times 10^8$ m/s is the speed of light, and $f_c = 5.9$ GHz is the carrier frequency.

A. PER

PER is defined as the ratio between the erroneously received packets and the total transmitted packets. It is the most common metric to indicate the reliability of a communication link and to characterize the receiver performance. The lower value of PER implies the higher reliability of a communication system. The PER curve is usually plotted on a logarithmic scale as a function of transmitted SNR.

For clarity and simplicity, only MCS 1 and MCS 5 are included in the simulation results. The PERs for the 100-byte and 1500-byte packets are shown in Fig.2 (a) and Fig.2 (b) for the urban NLOS scenario and in Fig.2 (c) and Fig.2 (d) for the highway NLOS scenario, respectively.

1) IMPACT OF ANTENNA CONFIGURATION

a: SISO

Since there is only one antenna at the transmitter and one antenna at the receiver, the SISO (1×1) system performs worst with the highest PER due to the lack of transmit diversity and receive diversity.

Moreover, the PER of the SISO system always decreases monotonically with the increase of SNR initially and reaches saturation finally, which is applicable for both scenarios, both packet sizes, and both MCSs.

b: MISO

With multiple transmit antennas and a single receive antenna, the transmit diversity is developed in the MISO (2×1) system and thus the PER is reduced compared to the SISO system.

Due to the absence of channel state information (CSI) at the transmitter, the performance of the MISO system is inferior to the SIMO system because of its higher PER even if the number of transmit antennas in the MISO system is equal to the number of receive antennas in the SIMO system [37], [58].

The occasional growth of PER with the increase of SNR emerges in the highway NLOS scenario with the 100-byte packet for MCS 1 and with the 1500-byte packet for both MCSs.

c: SIMO

Because of the advantage of the receive diversity, the SIMO (1×2) system, with multiple receive antennas and a single transmit antenna, is superior to both the MISO and SISO systems in terms of the further reduced PER.

The undesired rise of PER with the increase of SNR occurs in both scenarios with both packet sizes for MCS 5.

d: MIMO

Based on the full employment of both transmit diversity and receive diversity obtained by multiple transmit antennas and multiple receive antennas, the MIMO (2×2) system is optimal with the lowest PER among all the antenna configurations.

The abnormal increase of PER with the increase of SNR exists in the urban NLOS scenario with the 100-byte packet for MCS 5 and in the highway NLOS scenario with both packet sizes for both MCSs.

When the transmitter is far away from the receiver which results in the low SNR, the multi-antenna configuration is advantageous in mitigating the multipath components. Furthermore, the distinction of PER in the SISO, MISO, SIMO,

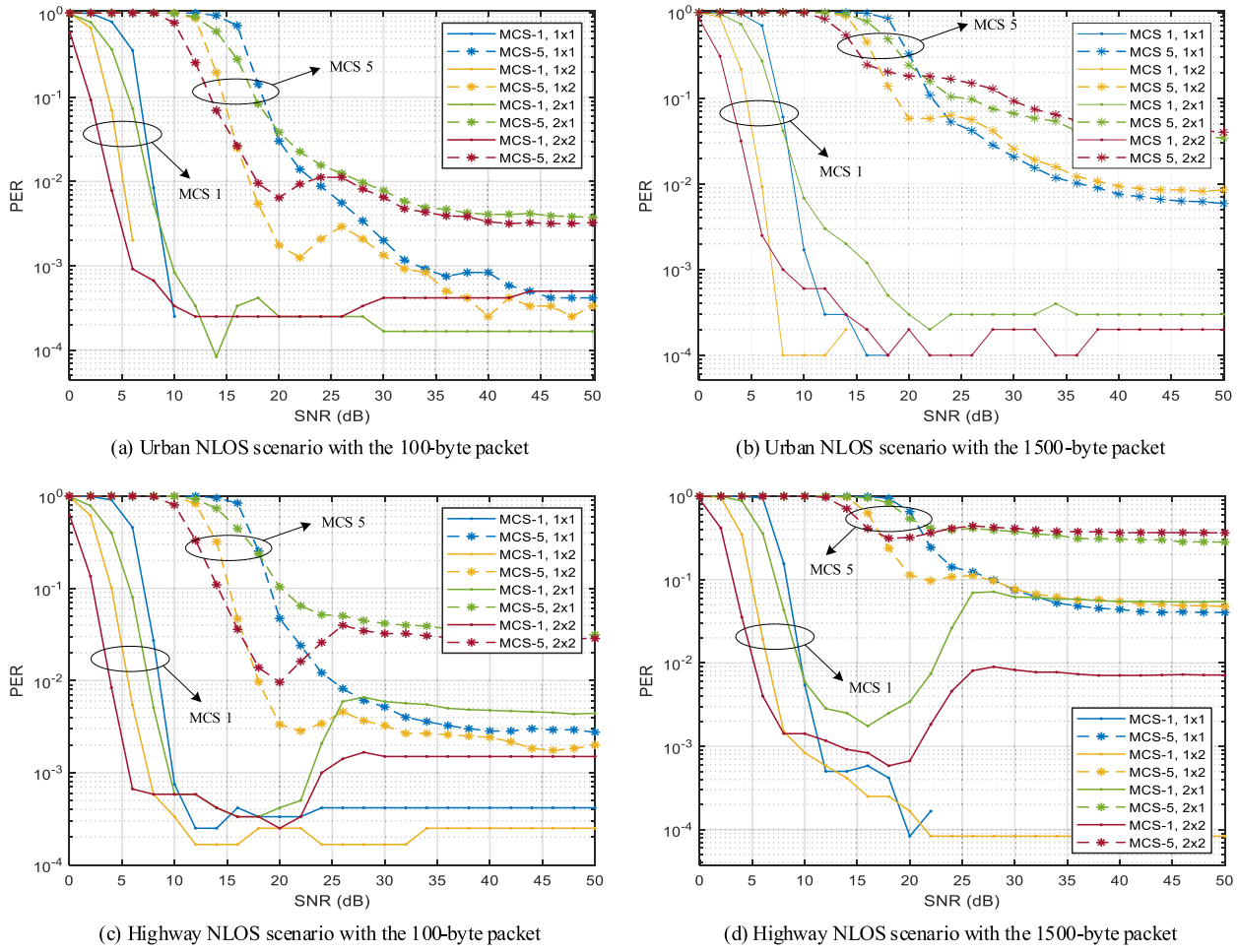

(a) Urban NLOS scenario with the 100-byte packet

(b) Urban NLOS scenario with the 1500-byte packet

(c) Highway NLOS scenario with the 100-byte packet

(d) Highway NLOS scenario with the 1500-byte packet

FIGURE 2. PER in urban NLOS and highway NLOS scenarios with the 100-byte and 1500-byte packets.

TABLE 6. SNR threshold (db) for PER.

V2V Scenario	100 bytes		1500 bytes	
	MCS 1	MCS 5	MCS 1	MCS 5
Urban NLOS	6	15.9	6.7	17.2
Highway NLOS	8	16.9	8.2	17.2

and MIMO systems can be observed below a specific SNR threshold which corresponds to a low-SNR range and thus a long-distance range. Specifically, the SNR thresholds of PER respectively for MCS 1 and MCS 5 with the 100-byte and 1500-byte packets under the urban NLOS and highway NLOS scenarios are listed in Table 6.

However, with the smaller distance between the transmitter and the receiver and thus the higher SNR, the multi-antenna interference becomes dominant. Hence, the abnormal increase of PER with the increase of SNR is not found in the SISO system but widely present under the MISO, SIMO, and MIMO systems instead. Furthermore, the saturated PER in certain multi-antenna systems, MISO, SIMO, or MIMO, can exceed that in the SISO system as the result of multi-antenna interference. The earliest minimum PER during the increase of SNR, the second maximum PER, and the ratio between them, which are combined to measure the temporary growth of PER, are shown in Table 7. The saturated PER at the highest SNR and its relative value compared to the earliest minimum PER are also provided as reference. In addition, the SNR at which the earliest minimum PER, the second maximum PER, and the saturated PER appear are given as well.

2) IMPACT OF V2V SCENARIO

a: URBAN NLOS SCENARIO

In the urban scenario with the slower movement of vehicles, the PER is generally monotonically decreasing with the increase of SNR until the occurrence of saturation. Exceptionally, there is an undesired rise of PER exclusively for MCS 5 in the 1×2 and 2×2 systems with the 100-byte packet and in the 1×2 system with the 1500-byte packet.

With the lower PER, the urban NLOS scenario with the lower Doppler effect is less sensitive to the larger packet size and the higher MCS.

The SNR threshold below which the PER of various systems can be distinguished is smaller than or equal to that in the highway NLOS scenario for MCS 1 and MCS 5, which indicates that the multi-antenna configuration is beneficial in

a smaller or equal low-SNR range and thus a smaller or equal long-distance range.

The PER of MCS 1 is equal to 0, which cannot be shown in the logarithmic-scale figure, with the 100-byte packet above 10 dB in the 1×1 system and above 6 dB in the 1×2 system respectively, and with the 1500-byte packet above 18 dB in the 1×1 system and above 14 dB in the 1×2 system respectively.

b: HIGHWAY NLOS SCENARIO

Due to a higher Doppler effect caused by the faster vehicles in the highway scenario, the PER is usually slightly higher than that in the urban NLOS scenario and the larger packet size and the higher MCS are less tolerable.

The abnormal increase of the PER is extensively present with both packet sizes for MCS 1 in the 2×1 and 2×2 systems and for MCS 5 in the 1×2 and 2×2 systems, and solely with the 1500-byte packet for MCS 5 in the 2×1 system.

The PER of MCS 1 equals to 0 and cannot be seen in the logarithmic-scale figure, above 22 dB in the 1×1 system with the 1500-byte packet.

3) IMPACT OF PACKET SIZE

a: 100-BYTE PACKET

The 100-byte packet mainly generates the smaller PER compared to the 1500-byte packet even if an occasional rise of PER is present, which is helpful to maintain a lower PER level and satisfy a higher reliability requirement. Moreover, the smaller packet is less influenced by the higher Doppler effect and the higher MCS. Hence, the smaller packet is recommended in the ultra-reliable communication, e.g., URLLC application.

Instead of the monotonic reduction with the increase of SNR, the temporary growth of PER occurs for MCS 5 in the 1×2 and 2×2 systems in both scenarios and for MCS 1 in the 2×1 and 2×2 systems in the highway NLOS scenario.

Moreover, with the lower SNR threshold, the smaller packet brings a smaller low-SNR range for the multi-antenna system to demonstrate its predominance.

The PER of MCS 1 can be as low as 0 in the 1×1 and 1×2 systems under the urban NLOS scenario.

b: 1500-BYTE PACKET

With the higher PER and thus the lower reliability, the degradation on the 1500-byte packet becomes even worse with the higher Doppler effect and the higher MCS.

The unusual rise of PER with the 1500-byte packet is similar to the 100-byte packet, except that the 2×2 system for MCS 5 in the urban NLOS scenario is excluded and the 2×1 system for MCS 5 in the highway NLOS scenario is included.

In addition to the 1×1 and 1×2 systems in the urban NLOS scenario, the PER of MCS 1 can also be reduced to 0 in the 1×1 system under the highway NLOS scenario.

4) IMPACT OF MCS

a: MCS 1

MCS 1 often realizes the lower PER and reaches a higher reliability in contrast with MCS 5, even with the existence of the unfavorable rise of PER. Besides, the lower MCS is less vulnerable to the higher Doppler effect and the larger packet size. Thus, the lower MCS is introduced for the more reliable and robust transmission.

Beginning with the monotonic decrease with the increasing SNR, the following PER undergoes the unexpected increase in the 2×1 and 2×2 systems with both packet sizes under the highway NLOS scenario.

In addition, the lower SNR threshold brought by the lower MCS reduces the low-SNR range over which the multi-antenna system is beneficial.

b: MCS 5

With the increased PER which lowers the reliability, the inferiority of MCS 5 compared with MCS 1 becomes more obvious for the higher Doppler effect and the larger packet size.

The destructive growth of PER emerges in the 1×2 and 2×2 systems with the 100-byte packet under both scenarios, in the 1×2, 2×1, and 2×2 systems with the 1500-byte packet under the highway NLOS scenario, and in the 1×2 system with the 1500-byte packet under the urban NLOS scenario.

Different from MCS 1 for which the PER can be sometimes decreased to 0, the PER can never be fallen to 0 for MCS 5.

The impact of all the parameters, including antenna configuration, V2V scenario, packet size, and MCS, on the PER are concluded in Table 8.

B. PRR

PRR is defined as the ratio of the successfully received packets to the total transmitted packets. Therefore, it is inversely related to PER and represents the probability of successful transmissions. The PRR curve is generally plotted on a non-logarithmic scale as a function of distance between the transmitter and the receiver. To evaluate the effective range of the communication technology, the maximum transmission range, i.e., transmission coverage, is defined as the distance where the link-level PRR value equals the desired PRR target, for example, 90%, for the reliability requirement.

Only MCS 1 and MCS 5 are involved in the simulation results for convenience. The PRRs for the 100-byte and 1500-byte packets are shown in Fig.3 (a) and Fig.3 (b) for the urban NLOS scenario and in Fig.3 (c) and Fig.3 (d) for the highway NLOS scenario, respectively.

1) IMPACT OF ANTENNA CONFIGURATION

a: SISO

Without the adoption of transmit diversity and receive diversity, the SISO (1×1) system is the least favorable with the lowest PRR and the smallest transmission coverage.

TABLE 7. Abnormal increase of PER with increase of SNR.

V2V Scenario	Packet Size	MCS	Antenna Configuration	Earliest Minimum PER (SNR)	Second Maximum PER (SNR)	Relative PER	Saturated PER (SNR)	Relative PER
Urban NLOS	100 bytes	MCS 5	SIMO	0.00125 (22 dB)	0.00292 (26 dB)	2.34	0.00033 (50 dB)	0.26
Urban NLOS	100 bytes	MCS 5	MIMO	0.00642 (20 dB)	0.01123 (24 dB)	1.75	0.00325 (50 dB)	0.51
Urban NLOS	1500 bytes	MCS 5	SIMO	0.0581 (20 dB)	0.0632 (24 dB)	1.09	0.0085 (50 dB)	0.15
Highway NLOS	100 bytes	MCS 1	MISO	0.00033 (16 dB/18 dB)	0.00658 (28 dB)	19.94	0.00442 (50 dB)	13.39
Highway NLOS	100 bytes	MCS 1	MIMO	0.00025 (20 dB)	0.00167 (28 dB)	6.68	0.0015 (50 dB)	6
Highway NLOS	100 bytes	MCS 5	SIMO	0.00283 (22 dB)	0.00458 (26 dB)	1.62	0.002 (50 dB)	0.71
Highway NLOS	100 bytes	MCS 5	MIMO	0.00956 (20 dB)	0.03971 (26 dB)	4.15	0.02853 (50 dB)	2.98
Highway NLOS	1500 bytes	MCS 1	MISO	0.00175 (16 dB)	0.07138 (28 dB)	40.79	0.05459 (50 dB)	31.19
Highway NLOS	1500 bytes	MCS 1	MIMO	0.00058 (18 dB)	0.00899 (28 dB)	15.5	0.00717 (50 dB)	12.36
Highway NLOS	1500 bytes	MCS 5	SIMO	0.0969 (22 dB)	0.11173 (26 dB)	1.15	0.04757 (50 dB)	0.49
Highway NLOS	1500 bytes	MCS 5	MISO	0.39216 (24 dB)	0.41322 (26 dB)	1.05	0.28169 (50 dB)	0.72
Highway NLOS	1500 bytes	MCS 5	MIMO	0.31348 (18 dB)	0.44053 (26 dB)	1.41	0.36364 (50 dB)	1.16

TABLE 8. Impact of parameters on PER.

Parameter	PER
Antenna Configuration	MIMO<SIMO<MISO<SISO (Below SNR threshold)
V2V Scenario	Urban NLOS<Highway NLOS (Mostly)
Packet Size	100 bytes<1500 bytes (Mostly)
MCS	MCS 1<MCS 5 (Mostly)

Furthermore, the PRR of the SISO system always experiences the monotonic increase with the decrease of distance and then remains stable for both MCSs with both packet sizes in both scenarios.

b: MISO

The PRR and coverage can be increased in the MISO (2×1) system which becomes preferable in comparison with the SISO system.

In accordance with the occasional growth of PER with the increase of SNR, the incidental reduction of PRR with the decrease of distance appears in the highway NLOS scenario for MCS 1 with both packet sizes and for MCS 5 with the 1500-byte packet.

c: SIMO

Depending on the further increased PRR and coverage, the SIMO (1×2) system is more beneficial than the MISO and SISO systems.

The unexpected drop of PRR with the decrease of distance happens for MCS 5 with both packet sizes under both scenarios.

d: MIMO

Due to the highest PRR and the largest coverage, the MIMO (2×2) system is the most advantageous in all the antenna configurations.

The harmful decline of PRR with the decrease of distance is present under the urban NLOS scenario for MCS 5 with the 100-byte packet and under the highway NLOS scenario for both MCSs with both packet sizes.

To estimate the coverage completely and consistently under different antenna configurations for the fixed Doppler effect, packet size, and MCS, the minimum coverage among the SISO, MISO, SIMO, and MIMO systems is selected as the basic coverage which represents the essential coverage for all the antenna configurations. Specifically, the basic coverages with respect to the 90% PRR requirement for MCS 1 and MCS 5 with the 100-byte and 1500-byte packets in the urban NLOS and highway NLOS scenarios are shown in Table 9.

Since the PERs of MCS 5 for the 2×1 and 2×2 systems are always above 10^{-1} in the highway NLOS scenario with the 1500-byte packet, the corresponding PRRs are always below 90% and the generality of the basic coverage for the 90% PRR target cannot be satisfied which disables its validity.

Contrary to the multi-antenna system which may result in the lower PRR and the smaller coverage due to the interference in the short-distance range compared to the SISO system, the multi-antenna configuration is helpful to overcome the multipath fading in the long-distance range and the

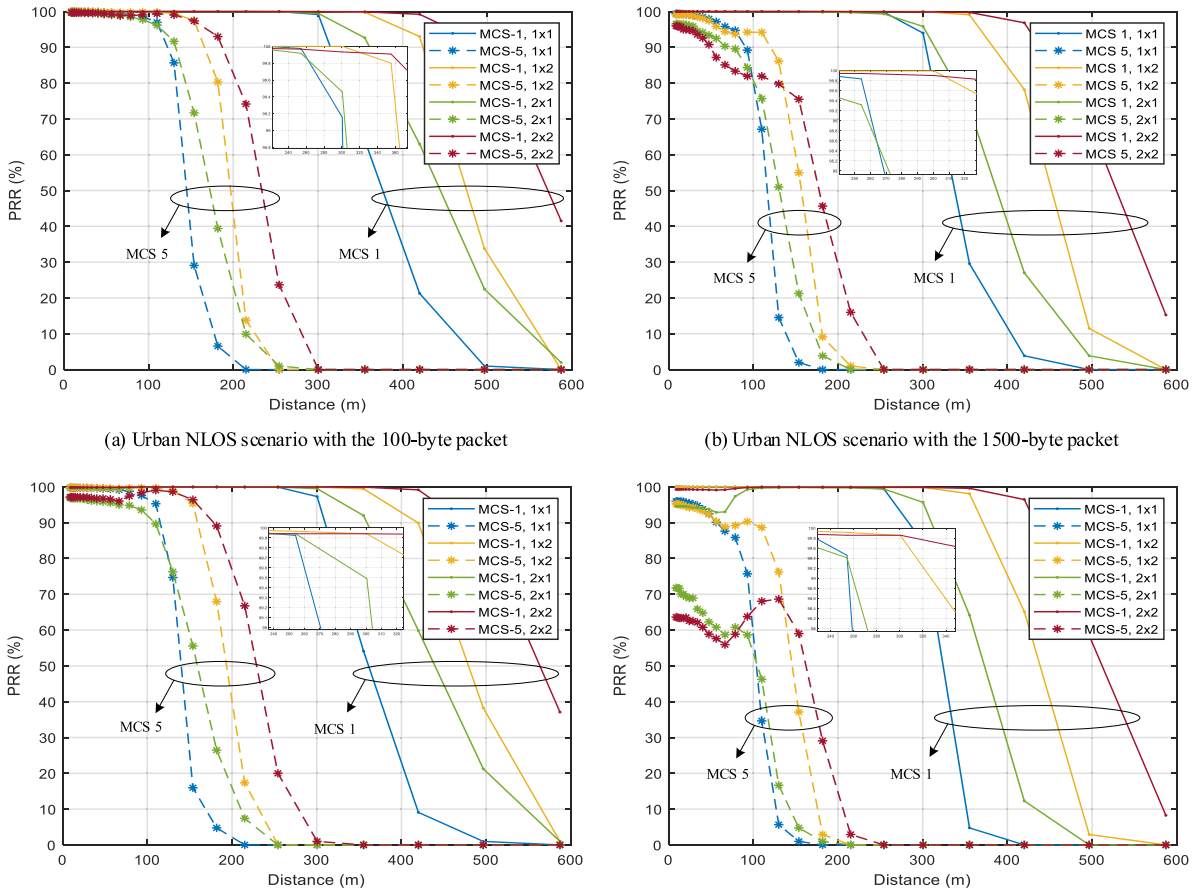

(a) Urban NLOS scenario with the 100-byte packet

(b) Urban NLOS scenario with the 1500-byte packet

(c) Highway NLOS scenario with the 100-byte packet

(d) Highway NLOS scenario with the 1500-byte packet

FIGURE 3. PRR in urban NLOS and highway NLOS scenarios with the 100-byte and 1500-byte packets.

TABLE 9. Basic coverage (m) with 90% PRR requirement.

V2V Scenario	100 bytes		1500 bytes	
	MCS 1	MCS 5	MCS 1	MCS 5
Urban NLOS	315	122	304	49
Highway NLOS	310	109	283	N/A

TABLE 10. Distance threshold (m) for PRR.

V2V Scenario	100 bytes		1500 bytes	
	MCS 1	MCS 5	MCS 1	MCS 5
Urban NLOS	321	154	307	136
Highway NLOS	300	137	295	136

difference of PRR in the SISO, MISO, SIMO, and MIMO systems can be distinguished above a specific distance threshold. Specifically, the distance thresholds of PRR respectively for MCS 1 and MCS 5 with the 100-byte and 1500-byte packets under the urban NLOS and highway NLOS scenarios are listed in Table 10.

2) IMPACT OF V2V SCENARIO

a: URBAN NLOS SCENARIO

Generally, the PRR undergoes the monotonic growth with the reduction of distance and enters the stability subsequently in the urban scenario with a lower Doppler effect. However, there is an unusual decline of PRR for MCS 5 in the 1×2 and 2×2 systems with the 100-byte packet and in the 1×2 system with the 1500-byte packet in agreement with the undesired rise of PER.

Less affected by the larger packet size and the higher MCS, the transmission coverage is less limited accompanied with the higher PRR. The basic coverage is always larger compared with the highway NLOS scenario due to the common extension on the coverage of each antenna configuration. Moreover, the basic coverage is still valid for 49 m even with the 1500-byte packet for MCS 5.

The distance threshold above which the PRR of various antenna configurations can be distinguished is larger than or equal to that in the highway NLOS scenario for MCS 1 and MCS 5 and hence generates a smaller or equal long-distance range within which the multi-antenna configuration is helpful.

b: HIGHWAY NLOS SCENARIO

The PRR, as well as the transmission coverage, is usually a bit smaller in the highway scenario than that in the urban scenario arising from the higher Doppler effect.

The unexpected drop of PRR occurs with both packet sizes for MCS 1 in the 2×1 and 2×2 systems and for MCS 5 in the 1×2 and 2×2 systems, and solely with the 1500-byte packet for MCS 5 in the 2×1 system.

The deterioration of the PRR with the 1500-byte packet for MCS 5 becomes more severe and the coverage is greatly restricted. Accordingly, the PRRs in the 2×1 and 2×2 systems are always below 90% and thus invalidate the basic coverage regarding the 90% PRR requirement.

3) IMPACT OF PACKET SIZE

a: 100-BYTE PACKET

Basically, the higher PRR and the larger coverage are obtained by the 100-byte packet in comparison with the 1500-byte packet. Hence, the basic coverage of all the systems is extended consequently. Besides, the smaller packet is less sensitive to the higher Doppler effect and the higher MCS and thus can fulfill a more rigorous PRR requirement. Faced with the most challenging environment, the highway NLOS scenario, there is still 109 m available in the basic coverage for MCS 5 with the 90% PRR target. Hence, the smaller packet is more favorable and more robust in the ultra-reliable communication where the large transmission coverage can be guaranteed.

In lieu of the monotonic increase with the decreasing distance, the casual reduction of PRR emerges for MCS 5 in the 1×2 and 2×2 systems under both scenarios and for MCS 1 in the 2×1 and 2×2 systems under the highway NLOS scenario.

In addition, the higher distance threshold for PRR with the smaller packet shortens the long-distance range over which the advantageous multi-antenna configuration is activated.

b: 1500-BYTE PACKET

As the result of the reduced PRR and coverage, the basic coverage is narrowed and even cannot be realized in the highway NLOS scenario for MCS 5 since the 1500-byte packet is more vulnerable to the higher Doppler effect and the higher MCS.

In comparison with the 100-byte packet, the abnormal decrease of PRR appears excluding the 2×2 system for MCS 5 in the urban NLOS scenario and including the 2×1 system for MCS 5 in the highway NLOS scenario.

4) IMPACT OF MCS

a: MCS 1

With the higher PRR and the larger coverage usually achieved by MCS 1, the basic coverage is accordingly enlarged in contrast with MCS 5. More resistant to the higher Doppler effect and the larger packet size, the basic coverage of 283 m can still be guaranteed even in the highway NLOS scenario with the 1500-byte packet. Thus, the lower MCS is superior in the reliability and robustness of the communication with the extension of transmission coverage.

TABLE 11. Impact of parameters on PRR.

Parameter	PRR
Antenna Configuration	MIMO>SIMO>MISO>SISO (Above distance threshold)
V2V Scenario	Urban NLOS>Highway NLOS (Mostly)
Packet Size	100 bytes>1500 bytes (Mostly)
MCS	MCS 1>MCS 5 (Mostly)

Other than the monotonic rise with the decrease of distance in the long-distance range, the undesired drop of PRR in the short-distance range happens in the 2×1 and 2×2 systems with both packet sizes under the highway NLOS scenario.

Additionally, the distance threshold of PRR for MCS 1 is greatly increased and hence the long-distance range which motivates the beneficial multi-antenna system is extremely reduced.

b: MCS 5

The PRR and coverage of MCS 5 descend more significantly, especially for the higher Doppler effect and the larger packet size. More seriously, the basic coverage in the highway NLOS scenario with the 1500-byte packet is disabled.

The accidental decline of PRR exists in the 1×2 and 2×2 systems with the 100-byte packet for both scenarios, in the 1×2, 2×1, and 2×2 systems with the 1500-byte packet for the highway NLOS scenario, and in the 1×2 system with the 1500-byte packet for the urban NLOS scenario.

The impact of all the parameters, including antenna configuration, V2V scenario, packet size, and MCS, on the PRR are concluded in Table 11.

C. EFFECTIVE DATA RATE

Due to the existence of PER in a real communication, the effective data rate of each MCS is calculated as the actual data rate multiplied by the probability of successful transmission, i.e., PRR, at each specified distance [5], [29].

Along with the change of distance between the transmitter and the receiver, the fading condition of the channel and its corresponding SNR are varying consequently. Hence, at each observed distance, the effective data rates of all MCSs are compared and their maximum is selected as the output effective data rate according to the link adaptation [28]. Since the higher actual data rate and the lower PRR are obtained by the higher MCS, while the lower actual data rate and the higher PRR are obtained by the lower MCS, all the MCSs are the candidates to reach the maximum product as the output effective data rate.

The output effective data rates for the 100-byte and 1500-byte packets are shown in Fig.4 (a) and Fig.4 (b) for the urban NLOS scenario and in Fig.4 (c) and Fig.4 (d) for the highway NLOS scenario, respectively.

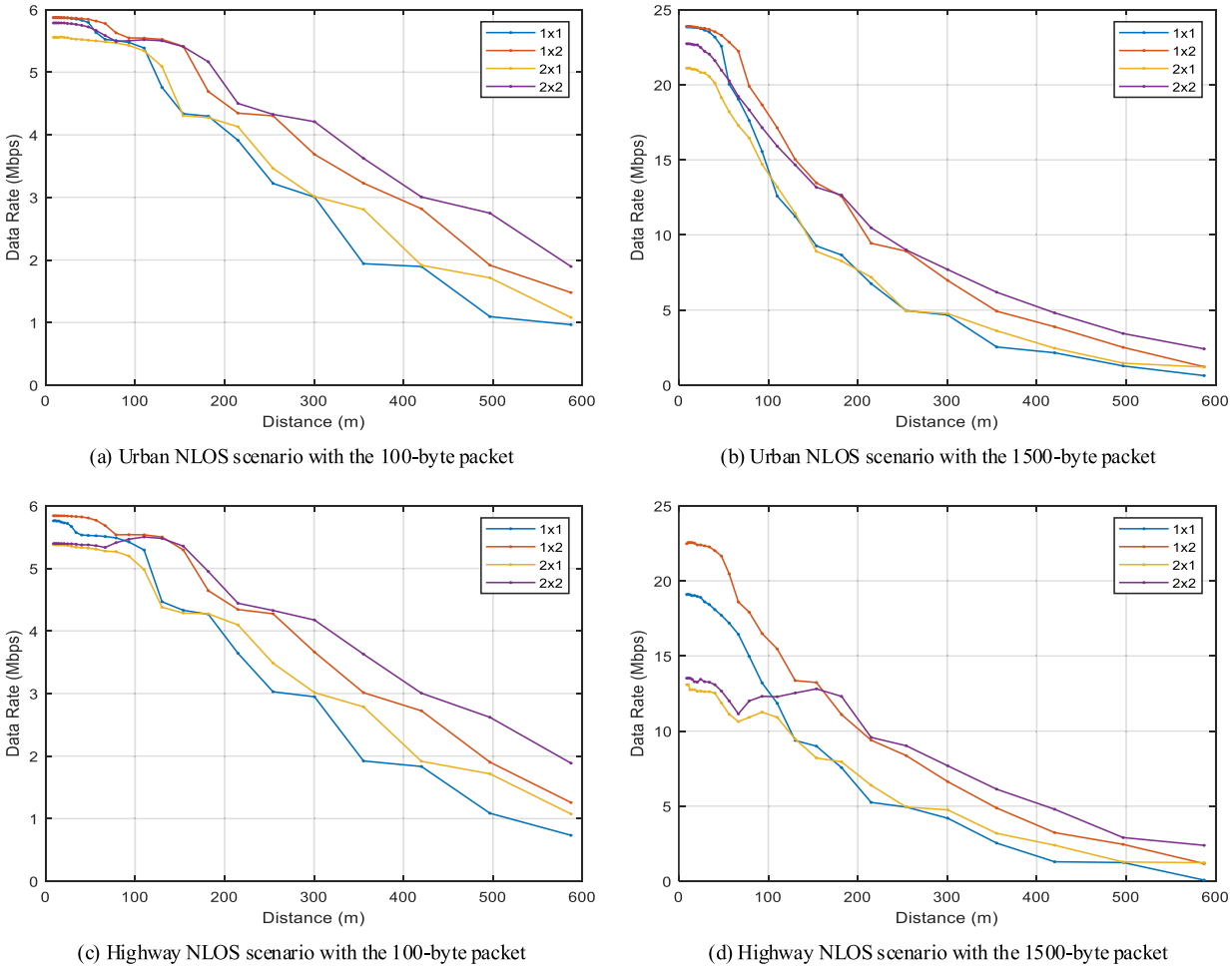

(a) Urban NLOS scenario with the 100-byte packet

(b) Urban NLOS scenario with the 1500-byte packet

(c) Highway NLOS scenario with the 100-byte packet

(d) Highway NLOS scenario with the 1500-byte packet

FIGURE 4. Output effective data rate in urban NLOS and highway NLOS scenarios with the 100-byte and 1500-byte packets.

1) IMPACT OF ANTENNA CONFIGURATION

a: SISO

The output effective data rate of the SISO (1 × 1) system always experiences the monotonic increase with the decrease of distance for both scenarios and both packet sizes and remains lowest among all the antenna configurations beyond a specific distance threshold.

b: MISO

The output effective data rate of the MISO (2 × 1) system is enhanced compared to the SISO system above the distance threshold. Except for the highway NLOS scenario with the 1500-byte packet where there is an obvious decline ranging from 93 m to 67 m, the data rate keeps monotonically increasing with the decreasing distance.

c: SIMO

The output effective data rate of the SIMO (1 × 2) system maintains the monotonic growth with the reduction of distance throughout both scenarios and both packet sizes and can be further elevated compared to the MISO as well as SISO systems beyond the distance threshold.

d: MIMO

The MIMO (2 × 2) system outperforms all the other systems with the highest output effective data rate above the distance threshold. Instead of the monotonic increase with the decline of distance which only occurs in the urban NLOS scenario with the 1500-byte packet, an evident reduction of the data rate exists in all the other three situations. Specifically, it is located from 110 m to 79 m in the urban NLOS scenario with the 100-byte packet, from 110 m to 67 m in the highway NLOS scenario with the 100-byte packet, and from 154 m to 67 m in the highway NLOS scenario with the 1500-byte packet, respectively.

Different from the interference which is generated by the multi-antenna system in the short distance and leads to the lower data rate of some multi-antenna systems compared with the SISO system, the multipath fading can be mitigated by the multi-antenna configuration at the farther distance defined by the threshold above which the data rate in the SISO, MISO, SIMO, and MIMO systems can be separated. Specifically, the distance thresholds of the output effective data rate respectively for MCS 1 and MCS 5 with the 100-byte and 1500-byte packets in the urban NLOS and highway NLOS scenarios are shown in Table 12.

TABLE 12. Distance threshold (m) for output effective data rate.

V2V Scenario	100 bytes	1500 bytes
Urban NLOS	185	198
Highway NLOS	177	173

2) IMPACT OF V2V SCENARIO

a: URBAN NLOS SCENARIO

The output effective data rate under the urban NLOS scenario is usually higher compared to the highway NLOS scenario, and the difference becomes more remarkable with the larger packet size. Hence, the urban NLOS scenario is less stringent than the highway NLOS scenario which becomes more obvious for the challenging larger packet.

Moreover, the larger distance threshold beyond which the data rate of various systems can be separated implies a smaller long-distance range where the multi-antenna configuration is advantageous.

b: HIGHWAY NLOS SCENARIO

The exacerbation of data rate compared with the urban NLOS scenario becomes even worse with the larger packet size. Specifically, the initial data rates of all the systems at the shortest distance in the urban NLOS scenario with the 1500-byte packet can remain higher than 20 Mbps, but in the highway NLOS scenario with the 1500-byte packet, except for the 1×2 system, the initial data rates of all the other three systems fall below 20 Mbps.

Different from the urban NLOS scenario where the undesired sink of data rate during the decrease of distance only exists in the 2×2 system with the 100-byte packet, the casual drop appears not only in the 2×2 system with the 100-byte packet but also in the 2×1 and 2×2 systems with the 1500-byte packet under the highway NLOS scenario.

3) IMPACT OF PACKET SIZE

a: 100-BYTE PACKET

The output effective data rate is lower with the 100-byte packet and generally undergoes the gradual increase with the decrease of distance. The unpopular drop is present in the 2×2 system under both the urban and highway NLOS scenarios. Less vulnerable to the higher Doppler effect, the difference between the urban and highway scenarios are notably suppressed.

The distance threshold is smaller in the urban NLOS scenario and larger in the highway NLOS scenario respectively, as the result of the optimal selection on all the MCSs.

b: 1500-BYTE PACKET

After the steep decrease with the increase of distance, the minimum data rate at the farthest distance becomes comparable to that with the 100-byte packet. However, the higher data rate over most of the distance range is still more beneficial for the high-throughput application.

TABLE 13. Impact of parameters on output effective data rate.

Parameter	Output Effective Data Rate
Antenna Configuration	MIMO>SIMO>MISO>SISO (Above distance threshold)
V2V Scenario	Urban NLOS>Highway NLOS (Mostly)
Packet Size	100 bytes<1500 bytes (Mostly)

The significant deterioration of the data rate is generated with the higher Doppler effect especially at the short distance within 200 m, and the temporary reduction with the decline of distance emerges in the 2×1 and 2×2 systems under the highway NLOS scenario.

The impact of all the parameters, including antenna configuration, V2V scenario, and packet size, on the output effective data rate are concluded in Table 13.

D. PACKET IAT

The packet IAT is defined as the time between two successive successful packet receptions. In a practical communication including PER, the packet IAT of each MCS is obtained by the packet transmission latency divided by the PRR at each appointed distance [28], [29].

Due to the variation of channel fading condition and its SNR caused by the changing distance, at each given distance, the packet IATs of all MCSs are compared and their minimum is selected as the output packet IAT by means of the link adaptation. Since the smaller transmission latency and the lower PRR are obtained by the higher MCS, whereas the larger transmission latency and the higher PRR are obtained by the lower MCS, all the MCSs are possible to realize the minimum quotient as the output packet IAT.

The output packet IATs for the 100-byte and 1500-byte packets are shown in Fig.5 (a) and Fig.5 (b) for the urban NLOS scenario and in Fig.5 (c) and Fig.5 (d) for the highway NLOS scenario, respectively.

1) IMPACT OF ANTENNA CONFIGURATION

a: SISO

The output packet IAT of the SISO (1×1) system, which always monotonically descends with the decline of distance for both packet sizes in both scenarios, keeps largest above the distance threshold.

Most sensitive to the higher Doppler effect and the larger packet size, the packet IAT is dramatically increasing with the growth of distance in the highway NLOS scenario with the 1500-byte packet and the resulting IAT at the farthest distance is as high as 165 ms.

b: MISO

The output packet IAT of the MISO (2×1) system is reduced in contrast with the SISO system beyond the distance threshold. The abnormal growth of the IAT only occurs in the

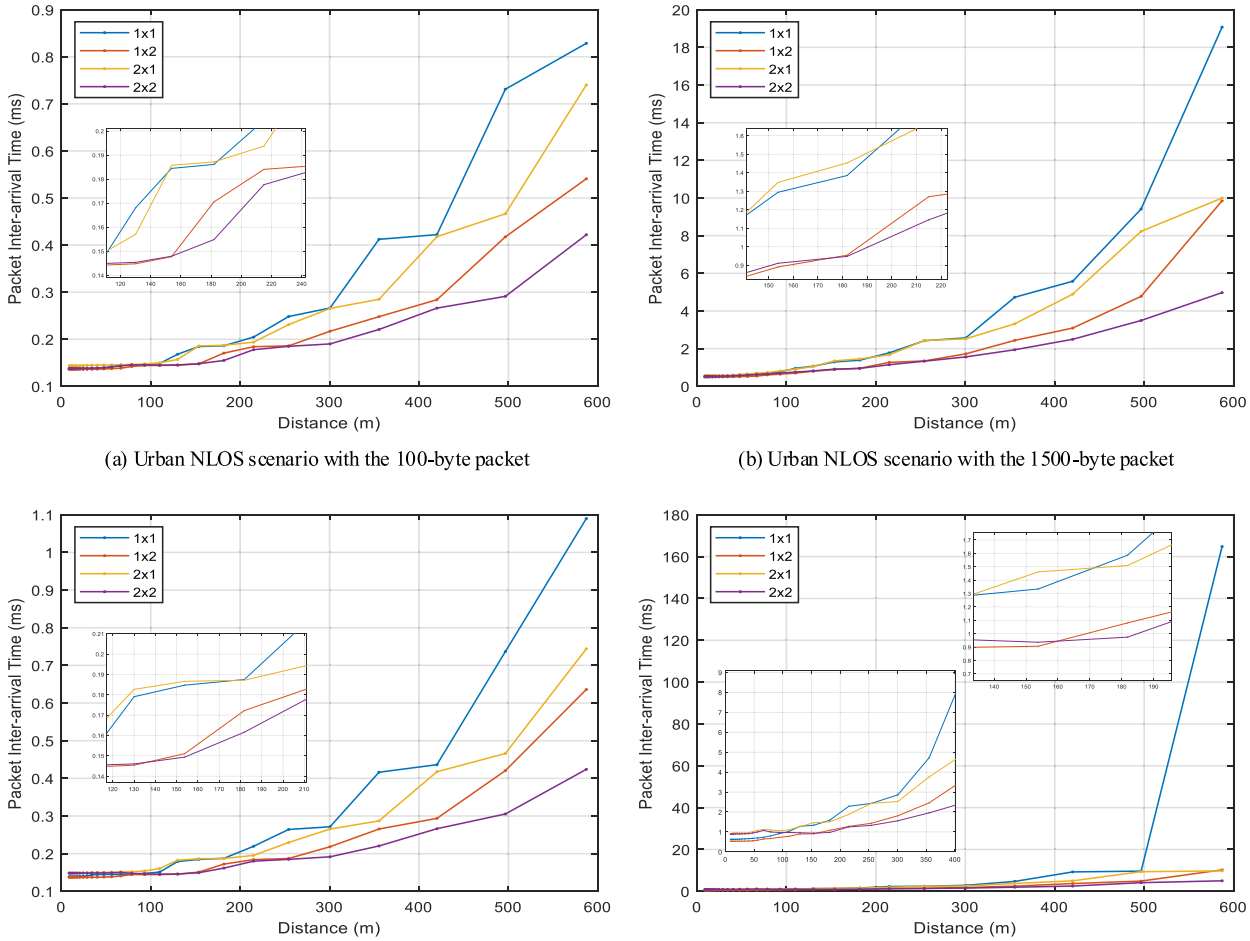

(a) Urban NLOS scenario with the 100-byte packet

(b) Urban NLOS scenario with the 1500-byte packet

(c) Highway NLOS scenario with the 100-byte packet

(d) Highway NLOS scenario with the 1500-byte packet

FIGURE 5. Output packet IAT in urban NLOS and highway NLOS scenarios with the 100-byte and 1500-byte packets.

highway NLOS scenario with the 1500-byte packet and is located between 93 m and 67 m, otherwise, the IAT maintains the monotonic reduction with the decrease of distance.

c: SIMO

Based on the monotonic drop with the decline of distance under both scenarios with both packet sizes, the output packet IAT of the SIMO (1×2) system can be further decreased compared with the MISO and SISO systems above the distance threshold.

d: MIMO

With the smallest output packet IAT beyond the distance threshold, the MIMO (2×2) system surpasses all the other systems. On one hand, the monotonic reduction of the IAT with the decreasing distance exclusively appears in the urban NLOS scenario with the 1500-byte packet. On the other hand, the unusual raise of the IAT extensively happens in all the other three instances where it is situated between 110 m and 79 m under the urban NLOS scenario with the 100-byte packet, between 110 m and 67 m under the highway NLOS scenario with the 100-byte packet, and between 154 m and 67 m under the highway NLOS scenario with the 1500-byte packet, respectively.

TABLE 14. Distance threshold (m) for output packet IAT.

V2V Scenario	100 bytes	1500 bytes
Urban NLOS	185	195
Highway NLOS	177	171

Regardless of the multi-antenna interference within the short distance which sometimes gives rise to the larger IAT of the multi-antenna systems in contrast with the SISO system, the multi-antenna configuration is still beneficial in overcoming the multipath fading at the longer distance where the IAT of the SISO, MISO, SIMO, and MIMO systems can be separated above the threshold. Accordingly, the distance thresholds of the output packet IAT respectively for MCS 1 and MCS 5 with the 100-byte and 1500-byte packets under the urban NLOS and highway NLOS scenarios are listed in Table 14.

TABLE 15. Impact of parameters on output packet IAT.

Parameter	Output Packet IAT
Antenna Configuration	MIMO<SIMO<MISO<SISO (Above distance threshold)
V2V Scenario	Urban NLOS<Highway NLOS (Mostly)
Packet Size	100 bytes<1500 bytes (Always)

2) IMPACT OF V2V SCENARIO

a: URBAN NLOS SCENARIO

The output packet IAT is generally smaller in the urban NLOS scenario than that in the highway NLOS scenario, and the gap increases for the larger packet size. Consequently, the urban NLOS scenario is more tolerant than the highway NLOS scenario which becomes more evident for the larger packet size.

Besides, the larger distance threshold above which the IAT of all the systems can be isolated confines the long-distance range where the advantage of the multi-antenna configuration can be initiated.

b: HIGHWAY NLOS SCENARIO

The growth of the IAT compared to the urban NLOS scenario is slight with the 100-byte packet but becomes more conspicuous with the 1500-byte packet, especially at the farthest distance in the 1×1 system which results in an incomparable IAT.

In addition to the 2×2 system with the 100-byte packet under the urban NLOS scenario, the abnormal rise of the IAT with the decline of distance occurs more widely in the highway NLOS scenario including the 2×2 system with the 100-byte packet and the 2×1 and 2×2 systems with the 1500-byte packet.

3) IMPACT OF PACKET SIZE

a: 100-BYTE PACKET

Always with the smaller output packet IAT which is favorable in the low-latency application, the reduction with the descending distance is gentle and the undesired increase exists in the 2×2 system for both scenarios. More robust to the higher Doppler effect, the deterioration of the IAT in the highway NLOS scenario is greatly alleviated.

The smaller distance threshold in the urban NLOS scenario and the larger distance threshold in the highway NLOS scenario are obtained according to the adaptation on all the MCSs.

b: 1500-BYTE PACKET

During the sharp growth of the IAT with the ascending distance, the resulting IAT is increased significantly compared to that with the 100-byte packet and the deviation between both scenarios becomes more prominent with the larger packet size. The abnormal growth of the IAT with the decreasing distance appears in the 2×1 and 2×2 systems under the highway NLOS scenario.

The impact of all the parameters, including antenna configuration, V2V scenario, and packet size, on the output packet IAT are concluded in Table 15.

V. CONCLUSION

In this paper, the PHY performance of IEEE 802.11bd is simulated and evaluated according to the PER, PRR, output effective data rate, and output packet IAT. The impact of diverse antenna configurations, i.e., SISO, MISO, SIMO, and MIMO, are demonstrated and compared. Both the urban NLOS and the highway NLOS scenarios are investigated and compared to explore their respective channel characteristics. The effect of different packet sizes and distinct MCSs are also taken into consideration. Some specific conclusions are as follows.

- The MIMO configuration with multiple transmit antennas and multiple receive antennas has a significant predominance in decreasing the PER, increasing the PRR as well as the transmission coverage, elevating the output effective data rate, and reducing the output packet IAT in comparison with the SIMO, MISO, and SISO configurations at the farther distance determined by the specific threshold. The SIMO system is superior to the MISO system even though the number of transmit antennas in the MISO system is equal to the number of receive antennas in the SIMO system, and the SISO system is least favorable with the worst performance.
- With the slight advantage in the lower PER, larger PRR as well as the transmission coverage, higher output effective data rate, and smaller output packet IAT, the urban NLOS scenario is more robust to the larger packet size and the higher MCS than the highway NLOS scenario.
- Due to the lower PER, larger PRR as well as the transmission coverage, and smaller output packet IAT, the smaller packet, which is less vulnerable to the higher Doppler effect and the higher MCS, is preferred in the high-reliability and low-latency communication. On the other hand, the larger packet can realize a higher output effective data rate and thus is recommended in the high-throughput communication.
- Based on the lower PER and larger PRR as well as the transmission coverage, the lower MCS, which is less sensitive to the higher Doppler effect and the larger packet size, is more beneficial for the high-reliability communication. The higher MCS selected in the link adaptation has the potential to achieve the higher output effective data rate for the high-throughput communication and the smaller output packet IAT for the low-latency communication.

According to the analysis on the simulation results, we can conclude that the utilization of multi-antenna configuration is indispensable to improve the quality of communication

at the farther distance. The urban NLOS scenario is more tolerant than the highway NLOS scenario with the slightly better performance. Moreover, both the packet size and the MCS need to be selected properly in terms of the trade-off among the high-reliability, high-throughput, and low-latency requirements.

REFERENCES

[1] G. Naik, B. Choudhury, and J.-M. Park, "IEEE 802.11bd & 5G NR V2X: Evolution of radio access technologies for V2X communications," *IEEE Access*, vol. 7, pp. 70169–70184, 2019.

[2] K. Kiela, V. Barzdenas, M. Jurgo, V. Macaitis, J. Rafanavicius, A. Vasjanov, L. Kladovscikov, and R. Navickas, "Review of V2X–IoT standards and frameworks for ITS applications," *Appl. Sci.*, vol. 10, no. 12, p. 4314, Jun. 2020.

[3] L. Cheng, B. E. Henty, D. D. Stancil, F. Bai, and P. Mudalige, "Mobile vehicle-to-vehicle narrow-band channel measurement and characterization of the 5.9 GHz dedicated short range communication (DSRC) frequency band," *IEEE J. Sel. Areas Commun.*, vol. 25, no. 8, pp. 1501–1516, Oct. 2007.

[4] X. Huang, D. Zhao, and H. Peng, "Empirical study of DSRC performance based on safety pilot model deployment data," *IEEE Trans. Intell. Transp. Syst.*, vol. 18, no. 10, pp. 2619–2628, Oct. 2017.

[5] W. Anwar, S. Dev, A. Kumar, N. Franchi, and G. Fettweis, "PHY abstraction techniques for V2X enabling technologies: Modeling and analysis," *IEEE Trans. Veh. Technol.*, vol. 70, no. 2, pp. 1501–1517, Feb. 2021.

[6] J. Choi, V. Marojevic, C. B. Dietrich, J. H. Reed, and S. Ahn, "Survey of spectrum regulation for intelligent transportation systems," *IEEE Access*, vol. 8, pp. 140145–140160, 2020.

[7] K. Ansari, "Joint use of DSRC and C-V2X for V2X communications in the 5.9 GHz ITS band," *IET Intell. Transp. Syst.*, vol. 15, no. 2, pp. 213–224, Feb. 2021.

[8] *IEEE Standard for Information Technology-Telecommunications and Information Exchange Between Systems Local and Metropolitan Area Networks-Specific Requirements—Part 11: Wireless LAN Medium Access Control (MAC) and Physical Layer (PHY) Specifications*, Standard 802.11-2020 (Revision of IEEE Std 802. 11-2016), 2020.

[9] V. Torgunakov, V. Loginov, and E. Khorov, "A study of channel bonding in IEEE 802.11bd networks," *IEEE Access*, vol. 10, pp. 25514–25533, 2022.

[10] W. Anwar, N. Franchi, and G. Fettweis, "A study on link adaptation techniques for IEEE 802.11bd based eV2X communications," in *Proc. IEEE 94th Veh. Technol. Conf. (VTC-Fall)*, Sep. 2021, pp. 1–7.

[11] *TSG SA, Release Description; Release 14*, document TR 21.914 V14.0.0, 3GPP, Jun. 2018.

[12] D. Garcia-Roger, E. E. González, D. Martín-Sacristán, and J. F. Monserrat, "V2X support in 3GPP specifications: From 4G to 5G and beyond," *IEEE Access*, vol. 8, pp. 190946–190963, 2020.

[13] *TSG SA, Release Description; Release 16*, document TR 21.916 V16.2.0, 3GPP, Jun. 2022.

[14] 5G Automotive Association. (Dec. 2017). *An Assessment of LTE-V2X (PC5) and 802.11p Direct Communications Technologies for Improved Road Safety in the EU*. [Online]. Available: https://5gaa.org/wp-content/uploads/2017/12/5GAA-Road-safety-FINAL2017-12-05.pdf

[15] 5G Automotive Association. (Oct. 2018). *V2X Functional and Performance Test Report; Test Procedures and Results*. 5GAA P-190033. [Online]. Available: https://5gaa.org/wp-content/uploads/2018/11/5GAA_P-190033_V2X-Functional-and-Performance-Test-Report_final-1.pdf

[16] 5G Automotive Association. (Oct. 2018). *V2X Technology Functional and Performance Benchmark Testing Key Findings*. [Online]. Available: https://5gaa.org/wp-content/uploads/2018/10/FCC-USDOT-CV2X-v2.14_wo_Video-c1_Final.pdf

[17] A. Bazzi, G. Cecchini, M. Menarini, B. M. Masini, and A. Zanella, "Survey and perspectives of vehicular Wi-Fi versus sidelink cellular-V2X in the 5G era," *Future Internet*, vol. 11, no. 6, p. 122, May 2019.

[18] *IEEE Guide for Wireless Access in Vehicular Environments (WAVE) Architecture*, Standard 1609.0-2019, 2019.

[19] F. Arena, G. Pau, and A. Severino, "A review on IEEE 802.11p for intelligent transportation systems," *J. Sensor Actuator Netw.*, vol. 9, no. 2, p. 22, Apr. 2020.

[20] B. Y. Yacheur, T. Ahmed, and M. Mosbah, "Analysis and comparison of IEEE 802.11p and IEEE 802.11bd," in *Communication Technologies for Vehicles*, F. Krief, H. Aniss, L. Mendiboure, S. Chaumette, and M. Berbineau, Eds. Cham, Switzerland: Springer, 2020, pp. 55–65.

[21] A. Triwinarko, I. Dayoub, and S. Cherkaoui, "PHY layer enhancements for next generation V2X communication," *Veh. Commun.*, vol. 32, Dec. 2021, Art. no. 100385.

[22] X. Ma and K. S. Trivedi, "SINR-based analysis of IEEE 802.11p/bd broadcast VANETs for safety services," *IEEE Trans. Netw. Service Manage.*, vol. 18, no. 3, pp. 2672–2686, Sep. 2021.

[23] T. Petrov, P. Pocta, and T. Kovacikova, "Benchmarking 4G and 5G-based cellular-V2X for vehicle-to-infrastructure communication and urban scenarios in cooperative intelligent transportation systems," *Appl. Sci.*, vol. 12, no. 19, p. 9677, Sep. 2022.

[24] T. Petrov, L. Sevcik, P. Pocta, and M. Dado, "A performance benchmark for dedicated short-range communications and LTE-based cellular-V2X in the context of vehicle-to-infrastructure communication and urban scenarios," *Sensors*, vol. 21, no. 15, p. 5095, Jul. 2021.

[25] J. Zhao, X. Gai, and X. Luo, "Performance comparison of vehicle networking based on DSRC and LTE technology," in *Proc. 6th Int. Conf. Intell. Transp. Eng. (ICITE)*, Z. Zhang, Ed. Singapore: Springer, 2022, pp. 730–746.

[26] V. Maglogiannis, D. Naudts, S. Hadiwardoyo, D. van den Akker, J. Marquez-Barja, and I. Moerman, "Experimental V2X evaluation for C-V2X and ITS-G5 technologies in a real-life highway environment," *IEEE Trans. Netw. Service Manage.*, vol. 19, no. 2, pp. 1521–1538, Jun. 2022.

[27] M. Karoui, A. Freitas, and G. Chalhoub, "Performance comparison between LTE-V2X and ITS-G5 under realistic urban scenarios," in *Proc. IEEE 91st Veh. Technol. Conf. (VTC-Spring)*, May 2020, pp. 1–7.

[28] W. Anwar, N. Franchi, and G. Fettweis, "Physical layer evaluation of V2X communications technologies: 5G NR-V2X, LTE-V2X, IEEE 802.11bd, and IEEE 802.11p," in *Proc. IEEE 90th Veh. Technol. Conf. (VTC-Fall)*, Sep. 2019, pp. 1–7.

[29] W. Anwar, A. Traßl, N. Franchi, and G. Fettweis, "On the reliability of NR-V2X and IEEE 802.11bd," in *Proc. IEEE 30th Annu. Int. Symp. Pers., Indoor Mobile Radio Commun. (PIMRC)*, Sep. 2019, pp. 1–7.

[30] R. Jacob, W. Anwar, N. Schwarzenberg, N. Franchi, and G. Fettweis, "System-level performance comparison of IEEE 802.11p and 802.11bd draft in highway scenarios," in *Proc. 27th Int. Conf. Telecommun. (ICT)*, Oct. 2020, pp. 1–6.

[31] B. Sun and H. Zhang. *802.11 NGV Proposed PAR*, Standard 802.11-18/0861r9, Nov. 2018.

[32] S. Zeadally, M. A. Javed, and E. B. Hamida, "Vehicular communications for ITS: Standardization and challenges," *IEEE Commun. Standards Mag.*, vol. 4, no. 1, pp. 11–17, Mar. 2020.

[33] R. Cao, H. Zhang, and P. Sharma, *Potential PHY Designs for NGV*, Standard 802.11-19/0016r0, Jan. 2019.

[34] B. Ahmed and M. A. Matin, *Coding for MIMO-OFDM in Future Wireless Systems*. New York, NY, USA: Springer, 2015, pp. 1–26.

[35] R. S. Kshetrimayum, *Fundamentals of MIMO Wireless Communications*. Cambridge, U.K.: Cambridge Univ. Press, 2017, pp. 1–11.

[36] L. Hanzo, Y. Akhtman, L. Wang, and M. Jiang, *MIMO-OFDM for LTE, Wi-Fi and WiMAX: Coherent Versus Non-Coherent and Cooperative Turbo-Transceivers*. Chichester, U.K.: Wiley, 2011, pp. 1–36.

[37] T. D. Chiueh, P. Y. Tsai, and I. W. Lai, *Baseband Receiver Design for Wireless MIMO-OFDM Communications*, 2nd ed. Singapore: Wiley, 2012, pp. 39–53.

[38] J. Yin, T. ElBatt, G. Yeung, B. Ryu, S. Habermas, H. Krishnan, and T. Talty, "Performance evaluation of safety applications over DSRC vehicular ad hoc networks," in *Proc. 1st ACM Int. Workshop Veh. Ad Hoc Netw.*, Oct. 2004, pp. 1–9.

[39] C. F. Mecklenbrauker, A. F. Molisch, J. Karedal, F. Tufvesson, A. Paier, L. Bernado, T. Zemen, O. Klemp, and N. Czink, "Vehicular channel characterization and its implications for wireless system design and performance," *Proc. IEEE*, vol. 99, no. 7, pp. 1189–1212, Jul. 2011.

[40] B. Sadeghi, *802.11bd Specification Framework Document*, Standard 802.11-15/0132r07, Sep. 2019.

[41] A. El-Keyi, T. ElBatt, F. Bai, and C. Saraydar, "MIMO VANETs: Research challenges and opportunities," in *Proc. Int. Conf. Comput., Netw. Commun. (ICNC)*, Jan. 2012, pp. 670–676.

[42] K. Raoof, M. B. Zid, N. Prayongpun, and A. Bouallegue, "Advanced MIMO techniques: Polarization diversity and antenna selection," in *MIMO Systems, Theory and Applications*, H. K. Bizaki, Ed. Norderstedt, Germany: BoD-Books on Demand, 2011, pp. 3–56.
[43] B. Kumbhani and R. S. Kshetrimayum, *MIMO Wireless Communications Over Generalized Fading Channels*. Boca Raton, FL, USA: CRC Press, 2017, pp. 1–70.
[44] R. W. Heath, Jr. and A. Lozano, *Foundations of MIMO Communication*. Cambridge, U.K.: Cambridge Univ. Press, 2019, pp. 77–110.
[45] L. Cazzella, D. Tagliaferri, M. Mizmizi, D. Badini, C. Mazzucco, M. Matteucci, and U. Spagnolini, "Deep learning of transferable MIMO channel modes for 6G V2X communications," *IEEE Trans. Antennas Propag.*, vol. 70, no. 6, pp. 4127–4139, Jun. 2022.
[46] D. J. Love and R. W. Heath, Jr., "Feedback techniques for MIMO channels," in *MIMO System Technology for Wireless Communications*, G. Tsoulos, Ed. Boca Raton, FL, USA: CRC Press, 2006, pp. 113–146.
[47] H. Huang, C. B. Papadias, and S. Venkatesan, *MIMO Communication for Cellular Networks*. New York, NY, USA: Springer, 2012, pp. 1–19.
[48] B. Clerckx and C. Oestges, *MIMO Wireless Networks: Channels, Techniques and Standards for Multi-Antenna, Multi-User and Multi-Cell Systems*, 2nd ed. Oxford, U.K.: Academic, 2013, pp. 1–27.
[49] S. Nijhawan, A. Gupta, K. Appaiah, R. Vaze, and N. Karamchandani, "Flag manifold-based precoder interpolation techniques for MIMO-OFDM systems," *IEEE Trans. Commun.*, vol. 69, no. 7, pp. 4347–4359, Jul. 2021.
[50] N. Hassan, D. A. Dupleich, C. Schneider, R. Thomä, and G. Del Galdo, "MIMO-TDL model parameter estimation from V2I channel sounding," in *Proc. 15th Eur. Conf. Antennas Propag. (EuCAP)*, Mar. 2021, pp. 1–5.
[51] M. Kahn, *V2V Radio Channel Models*, Standard 802.11-14/0259r0, Feb. 2014.
[52] E. Biglieri, R. Calderbank, A. Constantinides, A. Goldsmith, A. Paulraj, and H. V. Poor, *MIMO Wireless Communications*. Cambridge, U.K.: Cambridge Univ. Press, 2007, pp. 1–19.
[53] F. De Flaviis, L. Jofre, J. Romeu, and A. Grau, *Multi-Antenna Systems for MIMO Communications*. San Rafael, CA, USA: Morgan & Claypool, 2008, pp. 1–65.
[54] J. R. Hampton, *Introduction to MIMO Communications*. Cambridge, U.K.: Cambridge Univ. Press, 2014, pp. 1–69.
[55] Z. Hameed Mir and F. Filali, "LTE and IEEE 802.11p for vehicular networking: A performance evaluation," *EURASIP J. Wireless Commun. Netw.*, vol. 2014, no. 1, p. 89, May 2014.
[56] A. Bazzi, B. M. Masini, A. Zanella, and I. Thibault, "On the performance of IEEE 802.11p and LTE-V2V for the cooperative awareness of connected vehicles," *IEEE Trans. Veh. Technol.*, vol. 66, no. 11, pp. 10419–10432, Nov. 2017.
[57] A. Triwinarko, I. Dayoub, M. Zwingelstein-Colin, M. Gharbi, and B. Bouraoui, "A PHY/MAC cross-layer design with transmit antenna selection and power adaptation for receiver blocking problem in dense VANETs," *Veh. Commun.*, vol. 24, Aug. 2020, Art. no. 100233.
[58] A. J. Paulraj, D. A. Gore, R. U. Nabar, and H. Bolcskei, "An overview of MIMO communications—A key to gigabit wireless," *Proc. IEEE*, vol. 92, no. 2, pp. 198–218, Feb. 2004.

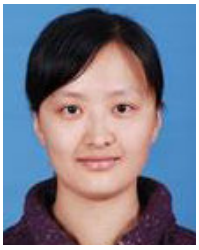

SHUTING GUO received the B.S.E. degree in electronic information engineering from Henan Normal University, Xinxiang, Henan, China, in 2004, and the M.S.E. degree in signal and information processing from Xidian University, Xi'an, Shanxi, China, in 2008. She is currently pursuing the Ph.D. degree in electrical engineering with Oakland University, Rochester, MI, USA.

Since 2008, she has been a Lecturer with the Electrical and Information Engineering College, Zhengzhou University of Light Industry, Zhengzhou, Henan. Her research interests include the physical layer evaluation and analysis on V2X communications with IEEE 802.11p, IEEE 802.11bd, LTE-V2X, and 5G NR.

DANIEL N. ALOI (Senior Member, IEEE) received the B.S., M.S., and Ph.D. degrees in electrical engineering from Ohio University, Athens, OH, USA, in 1992, 1996, and 1999, respectively.

He was a Research Assistant with the Avionics Engineering Center, School of Engineering and Computer Science, Ohio University, from 1995 to 1999; a Summer Intern with Rockwell International, Cedar Rapids, IA, USA; and a Senior Project Engineer with OnStar Corporation, a subsidiary of General Motors, from 2000 to 2002. He has been with the Electrical and Computer Engineering Department, Oakland University, Rochester, MI, USA, since 2002, where he is also the Founder and the Director of the Applied EMAG and Wireless Laboratory. He is a member of the Institute of Navigation. He has received in excess of $4M in research funding from a variety of federal and private entities, including the Federal Aviation Administration, the Defense Advanced Research Program Agency (DARPA), and the National Science Foundation (NSF). He has authored/coauthored over 100 technical papers and is an inventor on five patents. His research interests reside in area of applied electromagnetics, with an emphasis on antenna measurements, antenna modeling/analysis, and antenna design.

JIA LI (Senior Member, IEEE) received the B.S. degree in electronics and information systems from Peking University, Beijing, China, in 1996, and the M.S.E. and Ph.D. degrees in electrical engineering from the University of Michigan, Ann Arbor, MI, USA, in 1997 and 2002, respectively.

She has been a Faculty Member with the School of Engineering and Computer Science, Oakland University, since 2002. She has authored/coauthored over 90 refereed publications, including one book. Her past and current research are sponsored by NSF, NIH, General Motors, Fiat Chrysler, the National Research Council, and the Air Force Office of Scientific Research. Her research interests are in the areas of statistical learning and signal processing, with applications in radar, sensor fusion, communications, and biomedical imaging.

Dr. Li serves as a member for technical committees of several international conferences and workshops.

HONGMEI ZHAO received the B.S. degree in electrical engineering from the First Aviation University of Air Force, Xinyang, Henan, China, in 1999, and the Ph.D. degree in information and communication engineering from the Nanjing University of Science and Technology, Nanjing, Jiangsu, China, in 2009.

From 1999 to 2003, she was an Assistant Engineer with Technical Section, Luohe People's Broadcasting Station, Luohe, Henan. From 2009 to 2018, she was an Associate Professor with the Electrical and Information Engineering College, Zhengzhou University of Light Industry, Zhengzhou, Henan, where she has been a Professor, since 2018. From 2017 to 2018, she was a Visiting Scholar with the Electrical and Computer Engineering Department, The University of British Columbia, Vancouver, Canada. She is the author of two books, more than 40 articles, and 20 patents. Her research interests include the ultra-band indoor location systems, microstrip antenna, array signal processing, radio propagation, wireless navigation, and location technology application.

Dr. Zhao has four second awards of the Science and Technology Progress Awards of Henan Province and more than six first awards of the Outstanding Achievements in Science and Technology Award of Education Department of Henan.